

# Spectral Statistics of Irrational Polygonal Billiards

Hanya A. M. Ben Hamdin \*

Mathematics Department, Faculty of Science, Sirte University, Sirte, Libya

[hanyahamdin23@yahoo.com](mailto:hanyahamdin23@yahoo.com)

---

## Abstract

We investigate some statistical features of the spectrum related to the dynamical nature of the trajectories such as the fluctuation and the spacing between neighboring energy levels for polygonal billiard with some angles being irrational multiples of  $\pi$ . This addresses the effect of the polygonal geometry on the computed spectrum. .

**Keywords:** Quantum Chaos, Green function, Helmholtz equation, Polygonal Billiards, Nearest neighbour spacing distribution.

## 1. Introduction

---

The spectrum is a discrete set of numbers (eigenvalues) which are the allowed energies. Such a set provides more characteristic features and much more information than the continuous classical interval. The relation between the classical dynamics of a system and the spectral statistics is a rich area of research. One way to show the spectral statistics is Neighbour Spacing (NNS) distribution [1]; it is a statistical description of the spectrum in terms of the probability distribution of neighbouring level separations. It describes the tendency of the energy levels to cluster or repel depending on the nature of the underlying ray dynamics in phase space. The underlying classical ray dynamics of a system exhibits

---

\*Author for correspondence

a variety of dynamical classes ranging from complete integrability, such as the ray dynamics in ellipses and rectangles, through mixed systems with regular and chaotic regions such as mushroom and stadium billiards, to complete chaos such as the Sinai billiard [1, 2]. Respectively, the NNS distribution for integrable and chaotic systems follows Poisson and Wigner distributions [1, 2]. However, there are systems which are neither integrable nor fully chaotic nor mixed, and their energy levels show intermediate statistical properties between the Poisson and the Wigner distribution [3]. Such a phenomenon was observed for many systems such as the non hydrogenic atoms in a weak external field [3], and polygonal billiard with angles being rational multiples of  $\pi$  [4]. Richens and Berry state that the rational polygon (all angles equal rational multiples of  $\pi$ ) is a pseudo integrable system, i.e. its NNS distribution follows the semi-Poisson distribution [4]. Therefore the rational polygonal billiard is neither regular nor chaotic; it is an intermediate situation, where all trajectories belong to a surface of finite number of genus [4].

In addition, it is found other dynamical systems where the intermediate statistics are not the limiting case, but rather a transient phenomenon. For instance, the Kepler billiard, which is rectangular-shaped with specific potential, its NNS distribution is close to the semi-Poisson distribution at low energy [5]. However, with increasing the energy the NNS distribution tends to have the Poisson distribution [5]. Such a transient phenomenon also appears in the rough billiard, which is half-circular shaped with small deformations; its NNS distribution transits from the Poisson distribution through the semi-Poisson distribution to the Wigner distribution [5, 6].

In this paper we investigate the NNS distribution for a polygonal billiard with some angles being irrational multiples of  $\pi$ . This paper is structured as follows: in section 2 we set up the model and in section 3 we show how to apply the Boundary element Method (BEM) [7, 8] to the Helmholtz equation to construct the secular equation which we will use to compute the spectrum. In section 4, we compute the spectrum for a certain range of the wave number. Some statistical features related to the spectra of the polygonal billiard will be shown in sections (5) and (6). A conclusion is drawn in section 7.

## 2. Helmholtz Equation and its Fundamental Solution

---

For systems without potential such as free particle in a finite domain referred as quantum billiard problem, the stationary (time independent) Schrödinger equation can be reduced to the two-dimensional scalar Helmholtz equation with the scaling,

$$k = \left( \frac{\sqrt{2mE}}{\hbar} \right),$$

Where  $k$  is the wavenumber,  $m$  is the particle's mass,  $E$  is the particle's energy, and  $\hbar$  is the Planck constant. We consider the polygonal domain  $D$ , because such geometry is desired in many engineering applications, such as room acoustic. The homogeneous Helmholtz equation is given as

$$(\nabla_{\mathbf{q}}^2 + k^2)\psi(\mathbf{q}) = 0, \quad (1)$$

where  $\psi$  is the corresponding eigen function to the eigenvalue  $k$ , and  $\nabla^2$  is the two-dimensional Laplace operator in Cartesian coordinates. We set Dirichlet boundary conditions (DBC) on the boundary of  $D$ , that is

$$\psi(\mathbf{q}) = 0, \quad \text{for } \mathbf{q} \in \partial D.$$

To compute the eigenvalues of this eigenvalue problem, we will apply the BEM. The first step within the BEM formulations is to introduce the fundamental solution of the problem which is essential to establish the necessary boundary integral equations (BIEs). The fundamental solution of a differential equation is a solution with a unit point source equal to  $\delta(\mathbf{q} - \mathbf{r})$  applied at a given, fixed source point  $\mathbf{r}$ . The following equation thus holds,

$$(\nabla_{\mathbf{q}}^2 + k^2)G_0(\mathbf{q}, \mathbf{r}; k) = -\delta(\mathbf{q} - \mathbf{r}), \quad (2)$$

where the fundamental solution, also called the free-space Green function  $G_0$  defined as,

$$G_0(\mathbf{q}, \mathbf{r}; k) = \frac{i}{4} H_0^{(1)}(k|\mathbf{q} - \mathbf{r}|). \quad (3)$$

Physically,  $G_0(\mathbf{q}, \mathbf{r}; k)$  measures the response at a receiver point  $\mathbf{q}$  of a source point located at  $\mathbf{r}$  propagating into the free space, disregarding the prescribed boundary conditions. The function  $H_0^{(1)}(k|\mathbf{q} - \mathbf{r}|)$  denotes the Hankel function of the first kind and

zeroth order[9], and  $|\mathbf{q} - \mathbf{r}|$  is the distance between the source  $\mathbf{r}$  and the observation point  $\mathbf{q}$ .

### 3. Derivation of the Boundary Integral Equations

To derive the BIEs, one needs to multiply equation (1) and (2) by  $G_0(\mathbf{q}, \mathbf{r}; \mathbf{k})$  and  $\psi(\mathbf{q})$  respectively. Then subtract the two resulting equations, and integrate over the region  $D$  with an area element  $dA_q$ , to obtain

$$\iint_D [G_0(\mathbf{q}, \mathbf{r}; \mathbf{k}) \nabla_q^2 \psi(\mathbf{q}) - \psi(\mathbf{q}) \nabla_q^2 G_0(\mathbf{q}, \mathbf{r}; \mathbf{k})] dA_q = \iint_D \delta(\mathbf{q} - \mathbf{r}) \psi(\mathbf{q}) dA_q. \quad (4)$$

The integral on the right hand side (RHS) of equation (4) depends on the position of  $\mathbf{r}$ , and can be classified as the following,

$$\iint_D \delta(\mathbf{q} - \mathbf{r}) \psi(\mathbf{q}) dA_q = \begin{cases} \psi(\mathbf{r}), & \text{if } \mathbf{r} \in D; \\ \frac{1}{2} \psi(\mathbf{r}), & \text{if } \mathbf{r} \in \partial D; \\ 0, & \text{otherwise.} \end{cases} \quad (5)$$

For the left hand side (LHS) of equation(4), one needs to make use of the Green second identity [7, 8, 10] to obtain,

$$\int_{\partial D} \left( G_0(\mathbf{q}, \mathbf{r}; \mathbf{k}) \frac{\partial}{\partial n_q} \psi(\mathbf{q}) - \psi(\mathbf{q}) \frac{\partial}{\partial n_q} G_0(\mathbf{q}, \mathbf{r}; \mathbf{k}) \right) dq = \begin{cases} \psi(\mathbf{r}), & \text{if } \mathbf{r} \in D; \\ \frac{1}{2} \psi(\mathbf{r}), & \text{if } \mathbf{r} \in \partial D; \\ 0, & \text{otherwise,} \end{cases} \quad (6)$$

where  $\vec{n}_q$  denotes the outward unit normal vector at the boundary point  $q$ . The operator  $\frac{\partial}{\partial n_q}$  denotes the directional derivative along the normal vector  $\vec{n}_q$  at the boundary element  $q$ , that is,

$$\frac{\partial}{\partial n_q} G(\mathbf{q}, \mathbf{r}; \mathbf{k}) = \vec{n}_q \cdot \nabla_q G(\mathbf{q}, \mathbf{r}; \mathbf{k}),$$

where the dot denotes the scalar product,  $\nabla_{\mathbf{q}}$  is the gradient operator with respect to  $\mathbf{q}$ , and  $d\mathbf{q}$  is the arc length element along the boundary  $\partial D$ . The direct substitution of DBCs, and letting  $\mathbf{r} \rightarrow \beta \in \partial D$  in equation (6) leads to the following BIE,

$$\int_{\partial D} G_0(\mathbf{q}, \beta; \mathbf{k}) \frac{\partial}{\partial n_{\mathbf{q}}} \psi(\mathbf{q}) d\mathbf{q} = 0. \quad (7)$$

This BIE is classified as Fredholm integral equation of the first kind, because the unknown function  $\frac{\partial}{\partial n_{\mathbf{q}}} \psi(\mathbf{q})$  appears only implicitly, that is under the integration sign. Note that, this BIE has a logarithmically divergent kernel (weakly-singular) at  $\mathbf{q} = \beta$ . Actually, we can proceed with the BIE (9) after a careful treatment of the weak-singularity of  $G_0(\mathbf{q}, \beta; \mathbf{k})$ . But a well-known trick [10, 11] to avoid this additional complication is to take the normal derivative of the BIE (6) with respect to  $\mathbf{r}$  in the limit ( $\mathbf{r} \rightarrow \beta \in \partial D$ ) transforming all  $G_0$  terms

To  $\partial G_0 / \partial n_{\beta}$  terms. Since  $\mathbf{r}$  is an interior point, we may generally differentiate beneath the integral sign. That is applying the operator  $(\vec{n}_{\beta} \cdot \nabla_{\mathbf{r}})$  on (6), one obtains

$$\lim_{\mathbf{r} \rightarrow \beta} \frac{\partial}{\partial n_{\beta}} \psi(\mathbf{r}) = \lim_{\mathbf{r} \rightarrow \beta} \int_{\partial D} \left( \frac{\partial}{\partial n_{\beta}} G_0(\mathbf{q}, \mathbf{r}; \mathbf{k}) \frac{\partial}{\partial n_{\mathbf{q}}} \psi(\mathbf{q}) - \psi(\mathbf{q}) \frac{\partial}{\partial n_{\beta}} \frac{\partial}{\partial n_{\mathbf{q}}} G_0(\mathbf{q}, \mathbf{r}; \mathbf{k}) \right) d\mathbf{q}. \quad (8)$$

Since we aim to formulate a boundary only method, the interior field point is now positioned into the boundary  $\mathbf{r} \rightarrow \beta \in \partial D$  in equation (8). This should not present any restriction or difficulties and all the integrals remain well behaved as long as the source point is located far away from  $\beta$ . Imposing DBCs in equation (8) leads to,

$$\lim_{\mathbf{r} \rightarrow \beta} \frac{\partial}{\partial n_{\beta}} \psi(\mathbf{r}) = \lim_{\mathbf{r} \rightarrow \beta} \int_{\partial D} \frac{\partial}{\partial n_{\beta}} G_0(\mathbf{q}, \mathbf{r}; \mathbf{k}) \frac{\partial}{\partial n_{\mathbf{q}}} \psi(\mathbf{q}) d\mathbf{q}. \quad (9)$$

The RHS of equation (9) known in potential theory as the double layer potential, and there is a special relation for its limit to the boundary [10]. That is the kernel  $\lim_{\mathbf{r} \rightarrow \beta} \frac{\partial}{\partial n_{\beta}} G_0(\mathbf{q}, \mathbf{r}; \mathbf{k})$  has a jump when  $\mathbf{r}$  tends to the boundary. Therefore, when formulating the BIEs, it is necessary to consider the discontinuity properties for the layer potentials [10].

Take the limit  $\mathbf{r} \rightarrow \beta \in \partial D$  and apply the jump condition [10] for equation (9), one obtains,

$$\mu(\beta) = 2 \int_{\partial D} \mu(q) \frac{\partial}{\partial n_\beta} G_0(q, \beta; k) dq, \tag{10}$$

where,

$$\mu(q) = \frac{\partial}{\partial n_q} \psi(q).$$

This is a Fredholm equation of the second kind and its kernel is given as,

$$\frac{\partial}{\partial n_\beta} G_0(q, \beta; k) = \frac{ik}{2} \cos \theta(q, \beta) H_1^{(1)}(k|q - \beta|), \tag{11}$$

and

$$\cos \theta(q, \beta) = \frac{(q-\beta) \cdot \vec{n}}{|q-\beta|}, \quad \text{for } |q - \beta| \neq 0,$$

where  $\theta(q, \beta)$  is the angle between the normal at the boundary point  $\beta$  and the chord connecting the initial boundary point  $q$  to the final boundary point  $\beta$  as depicted in figure 1.

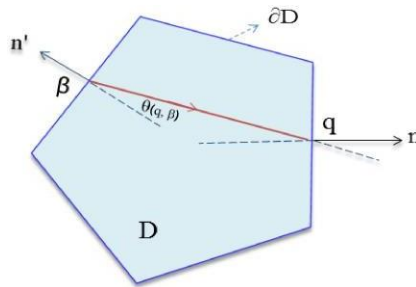


Figure 1. Sketch of the polygon with the boundary points  $q$  and  $\beta$ .

#### 4. The Secular Equation For the Spectrum

To obtain the eigenvalues condition, one needs to make use of the following property of the delta function,

$$\varphi(y) = \int_{-\infty}^{\infty} \delta(x - y) \varphi(x) dx. \tag{13}$$

So, the BIE (13) can be rewritten as,

$$\int_{\partial D} \left[ \delta(q - \beta) - 2 \frac{\partial}{\partial n_{\beta}} G_0(q, \beta; k) \right] \mu(q) dq = 0, \quad (14)$$

This BIE needs to be discretized on the boundary, thus we obtain the following condition,

$$\det[I - K(q, \beta; k)] = 0. \quad (15)$$

This is called the quantization condition, also it is known as the secular equation - a equation whose real zeros are in one to one correspondence with the spectrum. The values of  $k$  which satisfy equation (15) are the eigenvalues. The notation  $I$  denotes the identity matrix and  $K(q, \beta; k)$  is the boundary integral kernel defined for the boundary elements  $q$  and  $\beta$  as

$$K(q, \beta; k) = 2 \frac{\partial}{\partial n_{\beta}} G_0(q, \beta; k) = \frac{ik}{2} \cos \theta(q, \beta) H_1^{(1)}(k|q - \beta|) \quad (16)$$

where the boundary elements  $q$  and  $\beta$  will be suppressed thereafter.

The geometrical configuration of the polygonal domain for which we perform the computations of the spectrum has 5 angles  $(1/2)\pi$ ,  $(3/4)\pi$ ,  $(3/4)\pi$ ,  $0.397583618\pi$ ,  $0.602416382\pi$  as shown in figure 2. The calculation of the spectrum amounts to finding the zeros of the complex-valued determinant shown in figure 3 for a range of  $k$ . This can be achieved by finding the minima of  $|\det[I - K]|$ , to do so it is advantageous to make use of the singular value decomposition (SVD).

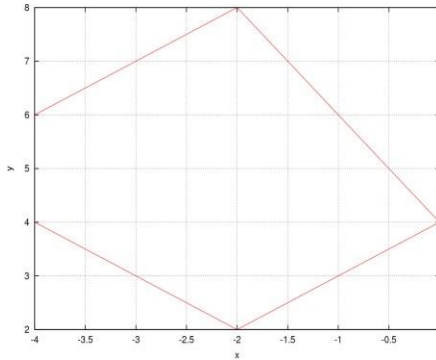


Figure 2. Sketch of the polygon used for computing the spectrum.

The spectral points (eigenvalues) are well defined by the sharp minima of the lowest singular values as a function of  $k$ . Using the SVD the determinant of the matrix  $(I - K)$  can be calculated by writing,

$$(I - K) = USV^\dagger$$

where  $V^\dagger$  denotes the conjugate transpose of  $V$ . The matrices  $U$  and  $V^\dagger$  are unitary matrices of  $n \times n$  dimension, and  $S$  is a diagonal matrix with real, non-negative elements  $S_1 \geq S_2 \geq \dots \geq S_n$

$S_n \geq 0$ . The set  $\{S_i\}_{i=1}^n$  is called the set of singular values in descending order. Hence the determinant can be calculated as

$$|\det(I - K)| = |\det U| |\det S| |\det V^\dagger|.$$

Since the modulus of the determinant of any unitary matrix equals unity, i.e.

$$|\det U| = |\det V^\dagger| = 1$$

Hence, one obtains

$$|\det(I - K)| = \prod_{i=1}^n S_{ii}$$

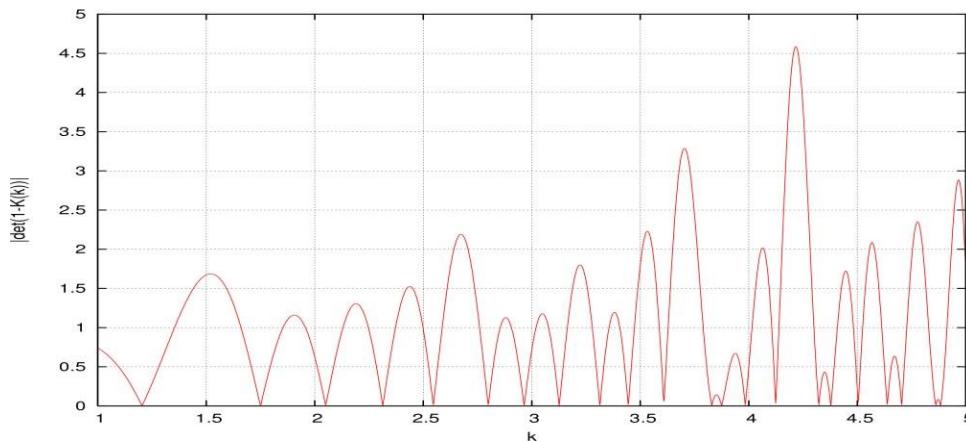


Figure 3. The modulus of the spectral determinant.

The advantage of making use of the SVD is that wherever there are minima of the second smallest singular value, this is a sign of the existence of two nearby eigenvalues as shown in figure 4. In this figure one can see that between  $k=25.38$  and  $k=25.4$ , there is minima of the second smallest singular value and there is two nearby eigenvalues.



Usually nearby eigenvalues are easy to miss in the computations. Figure 5 shows that only one of two nearby eigenvalues between 62.105 and 62.11 has been captured and the other was missed. So, one needs to increase the matrix size to capture nearby eigenvalues for higher range of  $k$  because the distance between successive eigenvalues decreases with increasing the wavenumber  $k$

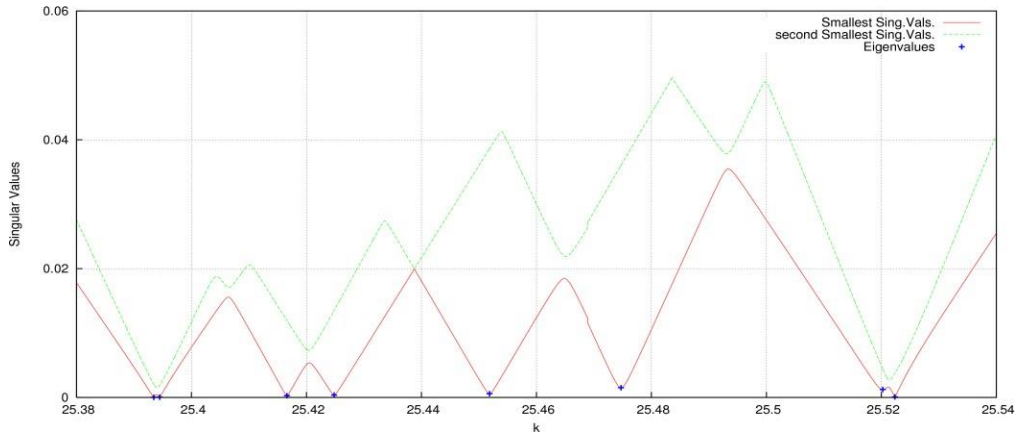


Figure 4. The solid and dashed lines respectively represent the smallest and second-smallest singular values, and the cross represents the eigenvalues.

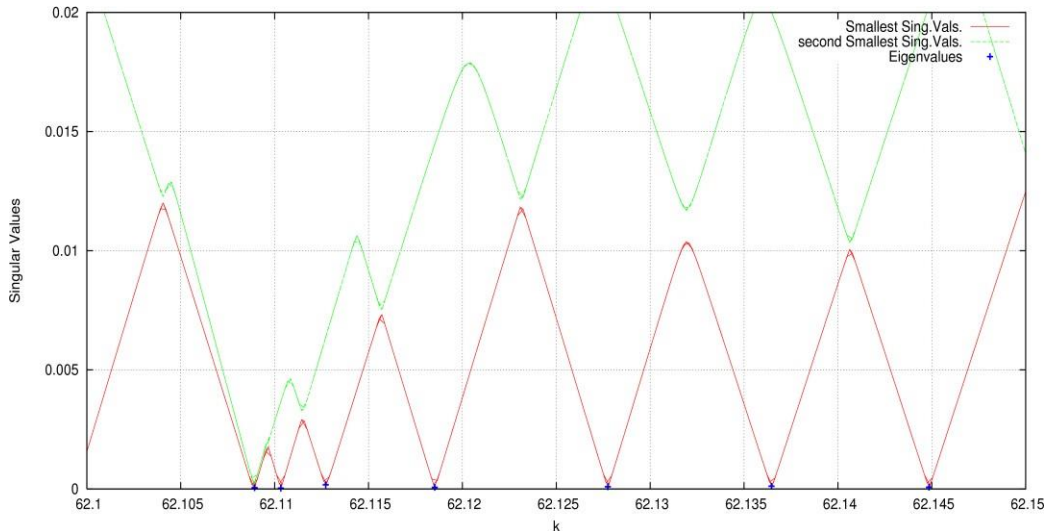


Figure 5. The solid and dashed lines respectively represent the smallest and second-smallest singular values, and the cross represents the eigenvalues. There is a missing eigenvalue just before  $k=62.11$

After obtaining the spectrum of about 5000 eigenvalues, still we need to check whether there were any missing eigenvalues. This check is usually can be achieved by looking into the oscillatory part of the density of state as shown next.

## 5. The Density of States and the Weyl Formula

---

We numerically compute the spectra of about 5000 eigenvalues with  $k < 62$  for a polygonal domain sketched in figure 2. Here we use this spectrum to compute the spectral density  $N(E)$ , which counts the number of energy levels below a given energy  $E$ ,

$$N(E) = \{N: E_n \leq E\}.$$

It can be written in terms of the wavenumber  $k$  as a sum of the smooth part and the oscillatory (fluctuating) part [1, 2] as,

$$N(k) = N_{osc} + N_{Weyl}$$

where  $N_{smooth} = N_{Weyl}$  is the mean part of the spectral counting function  $N(k)$ . It is also called the Weyl formula for the mode density which can for two-dimensional billiards shapes written as

$$N_{Weyl} = \frac{1}{4\pi} [Ak^2 - Lk] + c, \quad (17)$$

which consists of the area, length and curvature terms, where  $A$ ,  $L$  are the area and the perimeter of the domain, respectively. The geometric constant  $c$  denotes curvature and corners terms [2]. For smooth boundaries,  $c$  is dependent on the curvature of the boundary whereas for non-smooth boundaries  $c$  is dependent upon the angle of the corners [12]. The area term has an interpretation that the probability for the system to be in a certain region in phase space is proportional to the volume of such a region [2, 11].

Figure 6 shows that the Weyl term  $N_{Weyl}$  goes through the histogram of the cumulative density of eigenvalues  $N(E)$ .

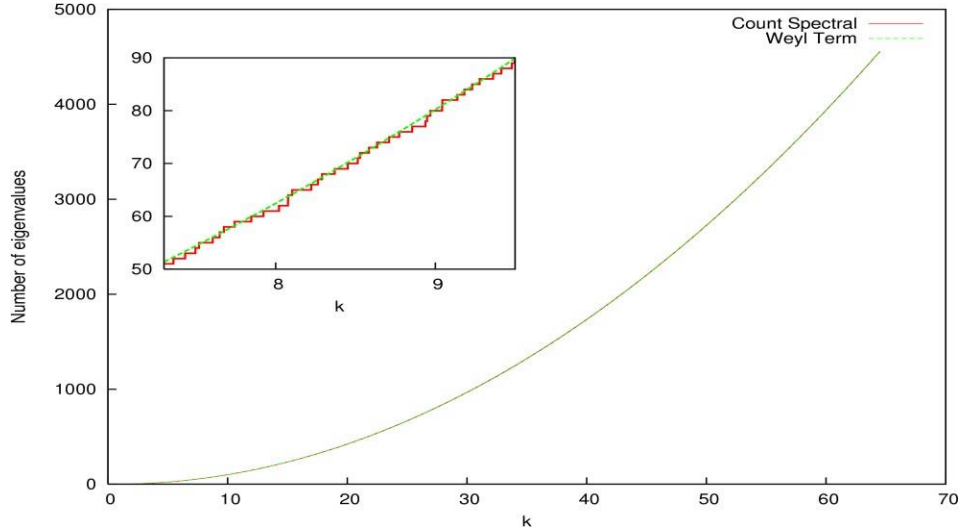


Figure 6. The spectral staircase counting function  $N(k)$  and its average, the Weyl term.

### 5.1 The oscillatory part of the density of states

A quantity which sensitively indicates whether spectral points were missed or not is the fluctuating part  $N_{osc}$  of the density of states. It is the difference between the staircase function  $N(k)$  counting the energy levels and the smooth part (Weyl term)  $N_{Weyl}$ , that is

$$.N_{osc} = \Delta N = N(k) - N_{Weyl}$$

Figure 7 shows that  $N_{osc}$  oscillates around zero, therefore it confirms that the spectrum is complete in the given range of  $k$ . A missing eigenvalue leads to an oscillatory signal as shown in figure 8. Therefore, the oscillatory part of the density of states offers check of obtaining the complete spectrum. Next we show some spectral statistics.

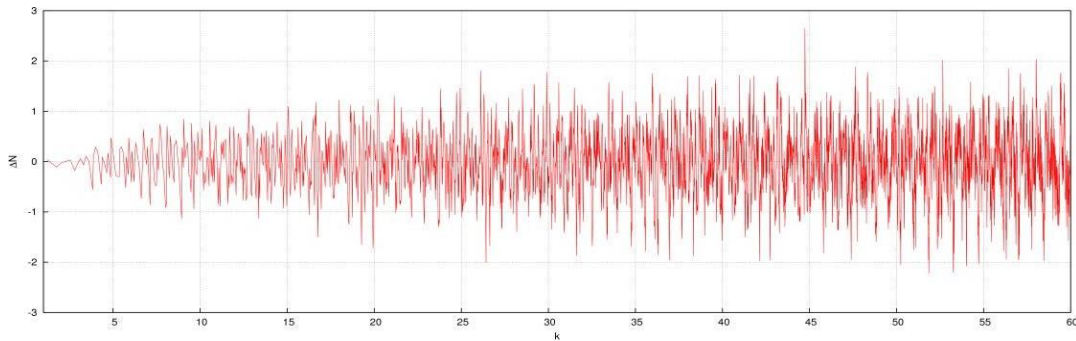


Figure 7. Fluctuating part of the density of states  $\Delta N$  for about 5000 eigenvalues.

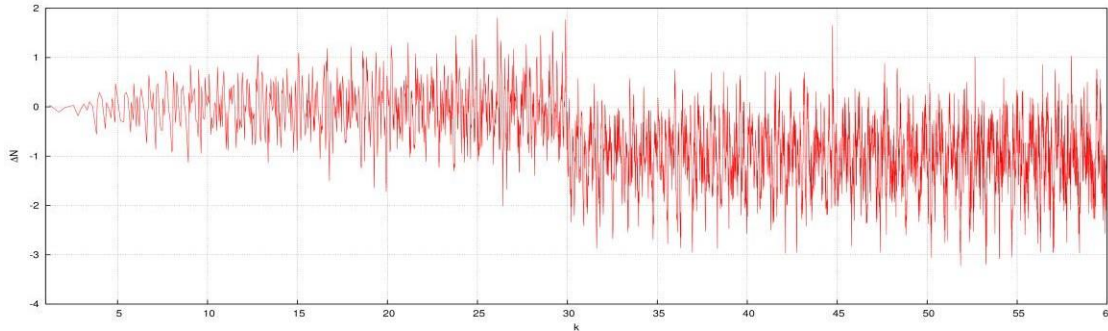


Figure 8. Fluctuating part of the density of states  $\Delta N$ , with missing an eigenvalue at  $k=30.012009$

## 6. Results and Discussion on the NNS Distribution

The nearest neighbour level spacing distribution is a spectral statistical description of neighbouring level separations. It describes the tendency of energy levels to cluster or repel depending on the nature of the underlying ray dynamics of the system. It measures the probability  $P(s)$  of finding the next energy level at distance  $s$  between two neighbouring energy levels for the unfolded spectrum. The spacing has been normalised to the mean spacing of 1, that is

$$\langle \Delta s \rangle = \langle E_{n+1} - E_n \rangle = 1$$

The spectra of different dynamical systems can only be compared if they are scaled in such a way.

Here we investigate the NNS distribution for the polygonal billiard with two angles being irrational multiple of  $\pi$ . From the numerical eigenvalues, we compute the level spacing and construct a histogram with boxes of width  $\Delta s = 0.08$  for the probability distribution  $P(s)$ . Then, at first we compare it against the Wigner distribution [1]. So, figure (9) shows that the NNS distribution for the irrational polygonal billiard has the standard property of Gaussian orthogonal ensembles (GOE) [1] which is defined as,

$$P_{\text{GOE}}(s) = \frac{\pi}{2} s e^{-(\pi/4)s^2};$$

This formula is known as the Wigner surmise for ensembles of random matrices [1].

Then we compare the NNS distribution for the polygonal billiard with some angles are equal irrational multiple of  $\pi$  against the semi-Poisson distribution which is defined as,

$$P_{SP}(s) = 4se^{-2s}.$$

Figures (9) and (10) on normal and logarithmic scale show that the NNS distribution for the polygonal billiard is described well by the Wigner distribution and deviates from the semi-Poisson distribution  $P_{SP}(s)$ .

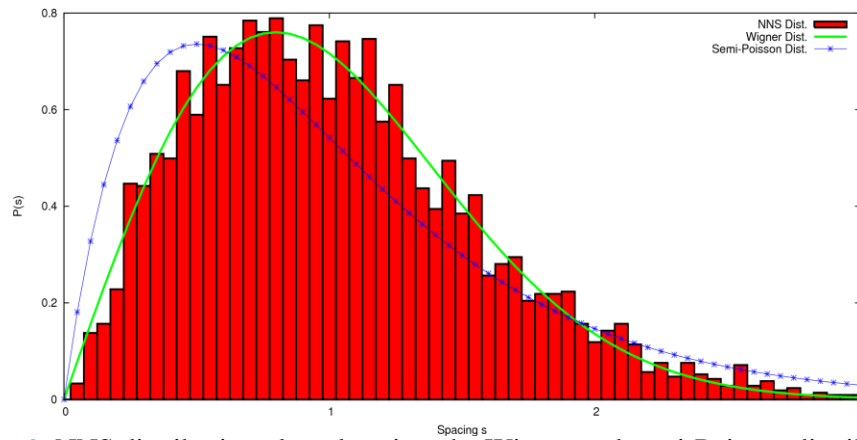


Figure 9. NNS distribution plotted against the Wigner and semi-Poisson distributions.

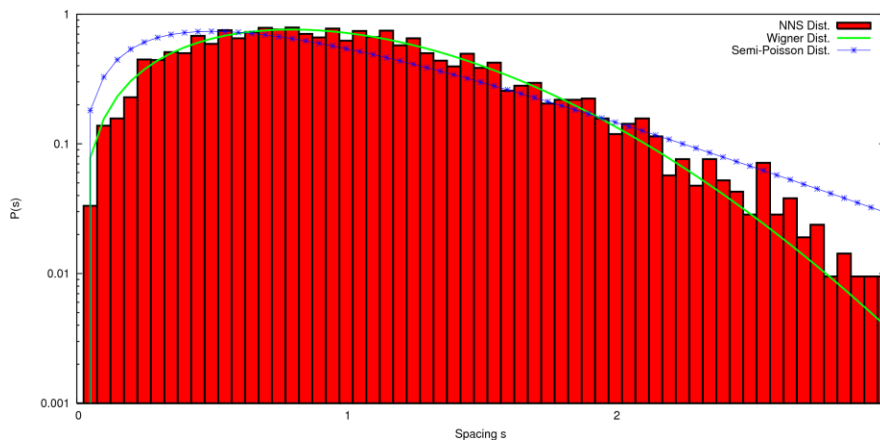


Figure 10. NNS distribution  $P(s)$  on logarithmic scale plotted against the Wigner and semi-Poisson distributions.

## 7. Conclusions

---

To summarize, we have numerically demonstrated that the level spacing distribution of the irrational polygonal billiard follows the Wigner distribution. It seems that the chaotic feature (non-integrability) of the motion in irrational polygonal billiards emerges from the divergence of a pair of neighbouring trajectories and the splitting of trajectories at a certain polygon corner. Within the configuration of the polygon for which we computed the spectrum there are two angles that are irrational multiples of  $\pi$ , so trajectories would bounce in all directions. This is potentially the reason why NNS distribution fits reasonably well and better with the Wigner distribution than the semi-Poisson distribution as shown above.

## 8. References

---

- [1] H. Stöckman, *Quantum Chaos: An Introduction*, Cambridge University, (1999).
- [2] G. Tanner and N Søndergaard, Wave Chaos in Acoustics and Elasticity, *J. Phys. A*, **40**, R443 (2007a).
- [3] T. Jonckheere, B.Grémaud, and D. Delande, Spectral Properties of Nonhydrogenic Atoms in Weak External Fields, *Phys. Rev. letters*, **81**, 12, 2442—2445 (1998).
- [4] P.Richens, and M. Berry, Pseudo-integrable systems in classical and quantum mechanics, *Physica 1D*, 495-512, (1981).
- [5] E. B. Bogomolny, U. Gerland, and C. Schmit, Models of intermediate spectral statistics, *Phys. Rev. E*, **59**, 2, (1999).
- [6] Y. Hlushchuk, A. BÇedowski, N. Savytskyy and L. Sirko , Numerical Investigation of Regimes of Wigner and ShnirelmanErgodicity in Rough Billiards , *PhysicaScripta***64**, 192–169 (2001).
- [7] C.A. Brebbia, J.C.F.Telles, and L. C. Wrobel.Boundary element techniques, Springer-Verlag, Berlin and New York, 1984.
- [8] C.A. Brebbia, Walker, The boundary element techniques in engineering, Newnas-Butterworths, London, 1979.
- [9] M. Abramowitz and A. Stegun, Handbook of Mathematical Functions, New York: Dover Publications, Inc., (1968).
- [10] R. Kress,Linear Integral Equations, Applied Mathematical Sciences; Vol. 82, Springer-Verlag, New York, Inc., second edition,(1999).
- [11] P. A. Boasman, Semiclassical Accuracy for Billiards, *Rev. Modern Phys.***74** (1992).
- [12] E. Bogomolny and E. Huges, Semiclassical Theory of Flexural Vibration of Plates, *Phys. Rev. A*, **57**, 4, 5404 (1998).